Local detection of electromagnetic energy transport below the diffraction limit in metal nanoparticle plasmon waveguides

Stefan A. Maier[*1], Pieter G. Kik[1], Harry A. Atwater[1], Sheffer Meltzer[2], Elad Harel[2], Bruce E. Koel[2], and Ari A.G. Requicha[2]

[1]Thomas J. Watson Laboratory of Applied Physics, California Institute of Technology, Mail Stop 128-95, Pasadena, California 91125, USA

[2]Laboratory for Molecular Robotics, Computer Science Department, University of Southern California, Los Angeles, California 90089, USA

*e-mail: stmaier@caltech.edu

Submitted: *exact date*

Correspondence should be addressed to:

Stefan A. Maier

California Institute of Technology

Mail-Stop 128-95

Pasadena, CA 91125, USA

e-mail: stmaier@caltech.edu

tel: 626 395 2193

fax: 626 229 7564

The miniaturization of optical devices to nanoscale dimensions requires structures that guide electromagnetic energy with a lateral mode confinement below the diffraction limit of light. This cannot be achieved using conventional waveguides {Saleh, 1991 #105} or photonic crystals {Mekis, 1996 #92}. However, it was suggested that electromagnetic energy can be guided below the diffraction limit along chains of closely spaced metal nanoparticles {Quinten, 1998 #91}{Brongersma, 2000 #108} that convert the optical mode into non-radiating surface plasmons {Kreibig, 1995 #103}. This enables the fabrication of functional optical devices with nanoscale dimensions {Brongersma, 2000 #108}{Maier, 2001 #10}. A variety of methods such as electron beam lithography {Maier, 2001 #10} and self-assembly {McMillan, 2002 #118} have been used to construct metal nanoparticle plasmon waveguides, however so far all investigations of their optical properties were confined to collective excitations {Krenn, 1999 #46}{Maier, 2002 #12;Maier, 2002 #14}, and direct experimental evidence for energy transport has proven elusive. Here, we present observations of electromagnetic energy transport over distances of about 0.5 μm in plasmon waveguides consisting of closely spaced silver rods. The waveguides are locally excited using the tip of a near-field optical microscope, and energy transport is probed using fluorescent nanospheres as local detectors.

The transport of electromagnetic energy in plasmon waveguides consisting of closely spaced metal nanoparticles relies on near-field coupling between surface plasmon-polariton modes of adjacent particles. This type of guiding due to near-field coupling has recently been demonstrated experimentally in macroscopic analogues operating in the microwave regime {Maier, 2001 #6}{Maier, 2001 #10}. At the submicron scale, theoretical and numerical analyses of plasmon waveguides were done, allowing for the

investigation of interparticle interactions {Quinten, 1998 #91} and the dispersion relation and group velocity for energy transport {Brongersma, 2000 #108}. The characteristics of optical pulse propagation in plasmon waveguides consisting of spherical or spheroidal nanoparticles were determined using finite-difference time-domain simulations {Maier, 2002 #15}. Far-field polarization spectroscopy experiments on ordered two-dimensional arrays of Au and Ag nanoparticles with submicron interparticle spacings have confirmed that electromagnetic interactions between the particles are present, revealing interparticle-distance dependent energy shifts of the collective plasmon resonances of the particle arrays {Lamprecht, 2000 #48;Salerno, 2001 #40}. It has further been shown that the resonance energy shifts that occur in one-dimensional arrays consisting of closely spaced Au particles can allow for an estimation of the group velocity and energy attenuation length of plasmon waveguides {Maier, 2002 #12;Maier, 2002 #14}. Energy attenuation lengths of 6dB/30nm were predicted for plasmon waveguides consisting of closely spaced spherical Au nanoparticles on an ITO substrate, and it was shown that a particle geometry change to spheroidal Ag particles should allow for an attenuation length increase to about 6dB/250nm {Maier, 2002 #14}. This kind of attenuation length is sufficient to allow detection of energy transport using local excitation.

Plasmon waveguides were fabricated using electron beam lithography with lift-off on ITO coated quartz slides, which allowed for a good control over particle size and spacing. The waveguide structures consist of rod-shaped Ag nanoparticles with dimensions of 90 nm x 30 nm x 30 nm and a surface-to-surface spacing of 50 nm between adjacent particles. The long axes of the individual nanoparticles were oriented perpendicular to the waveguide chain axis in order to allow for an increased near-field coupling between the

particles {Maier, 2002 #14}. The inset of Figure 1 shows a scanning electron micrograph of one of these plasmon waveguides. In order to allow for the determination of the plasmon resonances of the fabricated structures with a high signal-to-noise ratio using far-field spectroscopy, a large number of plasmon waveguides were arranged in a 100 μm x 100 μm grid with a grating constant of 1 μm as depicted in Figure 2b. It has previously been shown that cross talk between different waveguides is negligible for this grating constant {Maier, 2002 #12}. This way, far-field extinction spectra on these arrays reflect the properties of individual plasmon waveguides, and thus provide a probe of the near-field coupling between the nanoparticles comprising each waveguide.

Figure 1 shows the far-field extinction spectrum of the fabricated plasmon waveguides taken under normal incidence white light illumination with a spot size of 100 μm and a polarization along the long axis of the nanoparticles and thus perpendicular to the waveguide chain axis (red triangles). Also shown is the extinction spectrum of a grid of single Ag nanoparticles of the same geometry with an interparticle spacing of 1 μm, for which the interparticle coupling is negligible (black squares). The single particle extinction spectrum peaks at 2.18 eV for a polarization along the long particle axis, corresponding to a resonance wavelength of 570 nm. The extinction spectrum of the plasmon waveguide shows a resonance shift of about 100 meV to higher energies due to near-field coupling between the particles, in agreement with theoretical and numerical studies of plasmon waveguides {Brongersma, 2000 #108}{Maier, 2002 #15}. According to numerical simulations, this resonance shift of 100 meV translates into a maximum energy attenuation length on the order of 6dB/200nm for an excitation at the single particle resonance (2.18 eV in these samples), at which the energy transfer in a plasmon

waveguide is predicted to be most efficient independent of inter-particle spacing {Brongersma, 2000 #108}{Maier, 2002 #15}.

In order to directly probe energy transport in the fabricated plasmon waveguides, local excitation is necessary as opposed to far-field excitation of all particles in the arrays. To accomplish this, the tip of an illumination mode near-field optical microscope (Nanonics NSOM-100) is used as a local excitation source for nanoparticles in plasmon waveguides. In order to excite the mode of least damping, laser light from a dye laser at a wavelength of 570 nm, corresponding to the single particle resonance, was coupled into a multi-mode optical fiber attached to the Al-coated NSOM tip used for excitation. Figure 2a shows a schematic of our approach to excitation and energy transport detection. Power transport away from the directly excited nanoparticles in the plasmon waveguide is probed via the placement of polystyrene nanospheres filled with fluorescent molecules in close proximity to the waveguide structure. For this, the electron beam fabricated plasmon waveguide sample was coated with a thin poly-lysine layer, and the nanospheres were subsequently randomly deposited from an aqueous solution. The fluorescent dyes used show a strong absorption peaking at 580-590 nm near the plasmon resonance wavelength of a single fabricated Ag particle and emit radiation peaking at 610 nm. The excitation light is filtered out using a band pass filter, and the 610 nm dye emission is detected in the far-field with an avalanche photo diode. This scheme enables the observation of energy transport in the following way: first, energy is transferred from the illuminating tip to the plasmon waveguide. The excitation subsequently propagates along the nanoparticle structure and excites a fluorescent nanosphere placed on top of a waveguide at a sufficient distance from the excitation source. Energy transport would

result in dye emission even when the NSOM tip is located away from the dye, and thus would manifest itself in an increased spatial width of the fluorescence spot of a nanosphere attached to a plasmon waveguide compared to a single free nanosphere.

Figure 2c and 2d show simultaneously obtained topography and fluorescent NSOM scans of the control area outside the grid (Figure 2b, red box) with single nanospheres only and of the plasmon waveguide grid (Figure 2b, green box) together with fluorescent nanospheres, respectively. The samples were illuminated at the single particle resonance at 570 nm using a NSOM tip with a 100 nm aperture. The scan direction was perpendicular to the plasmon waveguides, and images were built up from left to right. The fluorescence NSOM spots of nanospheres located on top of plasmon waveguides were examined. In addition, NSOM scans of isolated nanospheres were used as a reference. Figure 2c shows the scan of the control area consisting of single nanospheres only, which was taken immediately before the scan of the plasmon waveguide area. Single nanospheres are clearly resolved in both the topography and the fluorescent NSOM image, with an arbitrary control particle highlighted (gray circle). Figure 2d shows the subsequent scan of a sample area comprising 4 plasmon waveguides in the left part of the image and fluorescent nanospheres. Two nanospheres (highlighted by red circles) are found to be located on top of plasmon waveguides, while one nanosphere at the right side of the scan area (gray circle) is positioned at a distance from a waveguide structure and can thus serve as a further control to ensure that the tip characteristics did not change during the scans. The widths of the fluorescence spots of both the two control nanospheres of Figure 2c and Figure 2d, respectively, and of the nanospheres attached to waveguides of Figure 2d were examined taking cuts through the NSOM data parallel to

the plasmon waveguide direction as highlighted in the fluorescent images (red and gray lines).

Figure 3 shows averages of five parallel cuts through each of the fluorescent nanosphere spots highlighted in Figure 2. Gaussian line shape fits to the data for both the control spheres (black and red lines and data points) and the two spheres attached to plasmon waveguides (green and blue lines and data points) are included. The fluorescent spots of the nanospheres attached to the plasmon waveguides show a full width at half maximum (FWHM) of 329 and 343 nm, respectively, compared to 174 and 193 nm for the control spheres. The control nanospheres scanned before and after the waveguide structures, respectively, show similar widths, confirming that the tip profile did not change appreciably during the scans.

The increase in the width of the nanosphere fluorescence of up to 170 nm for spheres attached to a plasmon waveguide structure can be attributed to local excitation of the plasmon waveguide, followed by energy transport along the waveguide toward the fluorescent dye particle. While for a free standing nanosphere the fluorescence signal decreases below the dark noise level if the tip is located approximately 200 nm away from the sphere center, a fluorescent nanosphere attached to a plasmon waveguide can be excited up to distances of 500 nm via the plasmon waveguide. We have thus obtained direct evidence for energy transport over this distance.

An energy attenuation length of a couple of hundred nanometers suggests the use of plasmon waveguides as functional end-structures in integrated optical devices. Further improvements of the interparticle coupling and the use of low loss substrates should allow for the fabrication of plasmon waveguides with larger energy attenuation lengths

and thus enable a wealth of highly integrated optical circuits operating below the diffraction limit.

In conclusion, we present experimental evidence for energy transport over 0.5 μm in plasmon waveguides consisting of rod-shaped silver nanoparticles using a local excitation and detection scheme employing near-field optical microscopy. Such waveguides provide a means for electromagnetic energy localization and manipulation below the diffraction limit and could be employed in future highly integrated optical devices.

Acknowledgements

The authors are grateful to Richard Muller, Paul Maker, and Pierre Echternach of the Jet Propulsion Laboratory in Pasadena for professional help with electron beam lithography. This work was sponsored by the NSF grant ECS0103543 and the Center for Science and Engineering of Materials at Caltech and the Air Force Office of Scientific Research.

The authors declare that they have no competing financial interests.

References:

Figure Captions:

Figure 1 (color) Far-field extinction spectrum of Ag nanoparticle chains and single particles. The far-field extinction spectrum of a plasmon waveguide consisting of Ag nanorods with a 3:1 aspect ratio and a surface-to-surface spacing of 50 nm between adjacent particles shows a plasmon resonance peak shift to higher energies (red triangles and Lorentz fit) compared to the extinction spectrum of isolated, non-interacting particles (black squares and Lorentz fit). The exciting light was polarized along the long axis of the nanorods, perpendicular to the particle chain axis. The inset shows an SEM micrograph of the plasmon waveguide under study.

Figure 2 (color) Near-field optical microscopy excitation and energy transport detection of plasmon waveguides. a, Sketch of the experiment. Light emanating from the tip of an illumination-mode near-field optical microscopy (NSOM) locally excites a plasmon waveguide. The waveguide transports the electromagnetic energy to a fluorescent nanosphere, and the fluorescence intensity for varying tip positions is collected in the far-field. b, SEM micrograph of a 100 x 100 micron grid consisting of Ag plasmon waveguides. c, d Topography and fluorescent NSOM scan of a 6 x 6 μm^2 area consisting of single fluorescent nanospheres (c, area highlighted by red box in b) and an area containing isolated fluorescent nanospheres in the vicinity of plasmon waveguides (d, area highlighted by green box in b). The fluorescent intensity of two single nanospheres (gray circles and data cuts A and B) can be compared to the intensity distribution of

nanospheres on top of plasmon waveguides (red circles, data cuts WG1 and WG2) using cuts (gray and red lines) through the fluorescent intensity scan along the waveguide axis.

Figure 3 (color) Evidence for energy transport in plasmon waveguides via the width of the intensity of fluorescent nanospheres. Shown are averages of five parallel cuts along the plasmon waveguide direction through the fluorescent spots highlighted in Figure 2 c, d for both single nanospheres (control A and B, black and red datapoints) and nanospheres located on top of plasmon waveguides (WG 1 and WG2, green and blue datapoints) as depicted in the inset. Gaussian line shape fits to the data show an increased width for nanospheres located on plasmon waveguides.

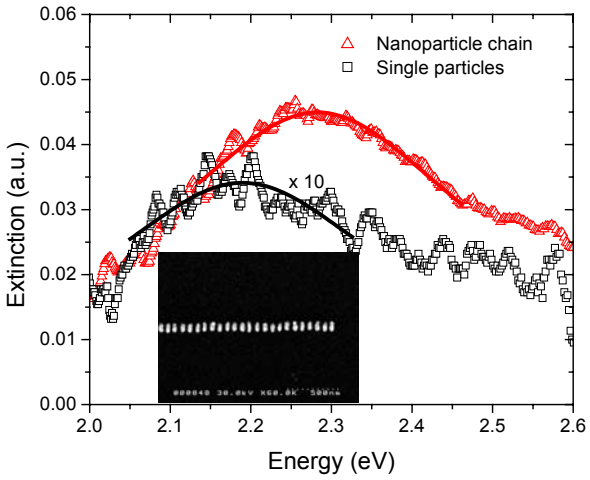

Figure 1 (color) of 3

Stefan A. Maier, submitted to Nature Materials

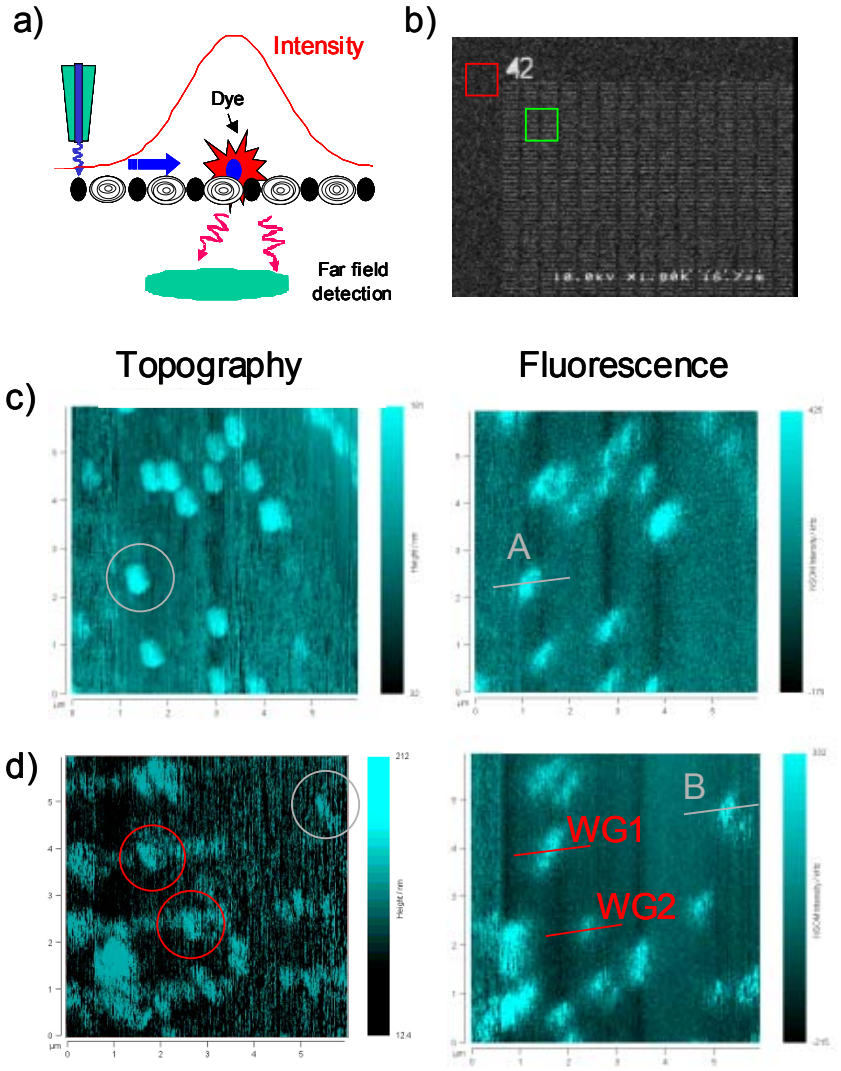

Figure 2 (color) of 3

Stefan A. Maier, submitted to Nature Materials

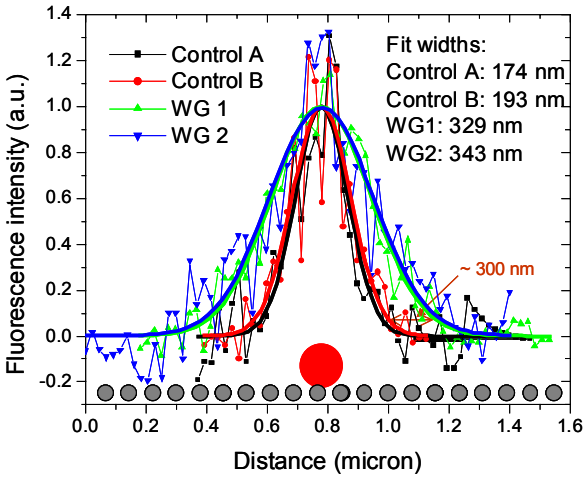

Figure 3 (color) of 3

Stefan A. Maier, submitted to Nature Materials